

Illumination-Invariant Target Color Detection for EMCCD Camera

Min-Sung Kang, Chang-Beom Oh, and Kwang-Hoon Sohn; School of Electrical & Electronic Engineering, Yonsei University, Korea

Abstract

We introduce an illumination-invariant target color detection technique for EMCCD camera. The EMCCD camera has an advantage to acquire a color image even though the surroundings are very low-light-levels. Since the EMCCD amplifies the input signal, an EMCCD noise which is caused by the gain process in low-light imaging systems occurs. In order to use the EMCCD image, we firstly reduce the noise by using selective Gaussian blur filter which maintains the image boundary. The threshold for the Gaussian blur filter is decided after the noise analysis by using sample patch modeling. We use illumination-invariant color space based on the image acquisition model for the target color detection. Experimental results show a good possibility to apply to intelligent surveillance system and night vision system.

Introduction

Image acquisition in low-light-level conditions has become a critical issue, especially in surveillance applications. Recently, there have been some hardware advances in low light imaging such as an intensified CCD (ICCD), electron-bombarded CCD (EBCCD), and electron multiplying CCD (EMCCD). In particular, the EMCCD is capable of providing useful performance in very low-light-level conditions, in which either intensified or slow-scan sensors were previously used [1-3]. The EMCCD produces gain through impact ionization by adding a multiplication or gain register to the output register. The advantage of the EMCCD is that the gain is applied prior to readout, thus minimizing the deleterious effects of readout noise in low-light-level conditions [4,5]. So the EMCCD can be a solution of low-light-level imaging, such as night vision system [6,7]. However, the EMCCD image shows some drawback in noise occurrence [8].

The methodology for illumination-invariant target color detection is summarized in Fig. 1. We model the image noise which is caused by signal multiplying of EMCCD by using polynomial fitting method with Gaussian kernel. The standard deviation result of the noise modeling affects a threshold decision of selective Gaussian blur noise reduction (SGBNR) [9]. We convert the input image to the illumination invariant color space [10]

EMCCD Image Analysis

The EMCCD image has advantage to acquire color image in very low-light-level conditions. For example, the images which are acquired from general CCD sensor camera and EMCCD sensor camera in various low-light-level conditions are shown as Fig. 2. The EMCCD sensor is able to acquire color information in low-light-level conditions, the CCD sensor, on the other side, cannot obtain fine color information.

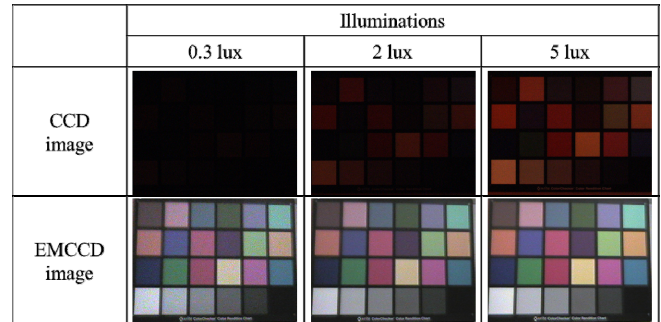


Figure 2. Comparison the EMCCD image with the CCD image in low-light-level conditions

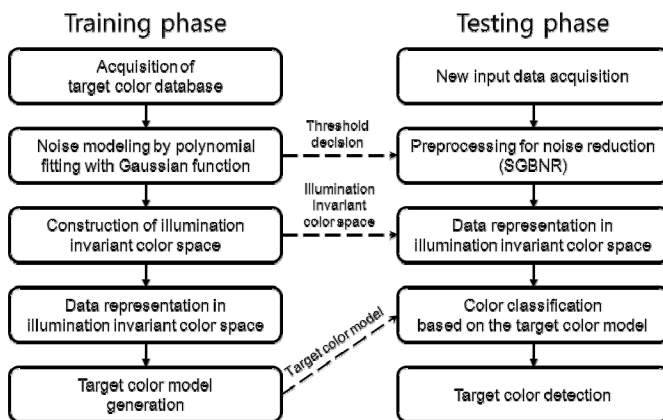


Figure 1. Flowchart of illumination invariant target color detection

In order to remove the EMCCD noise from the image, we firstly analyze the GretagMacbeth ColorChecker image which is captured by the EMCCD camera in low-light-level conditions. We select the middle-level grey patch for the EMCCD noise analysis because it has almost same RGB values and doesn't make saturation. For the EMCCD noise analysis, firstly we suppose that the EMCCD noise will be occurred as a Gaussian form. Therefore, we model the middle-level grey patch by using polynomial fitting method with Gaussian kernel. Equation (1) is Gaussian function.

$$y = H \exp\left(\frac{-(x - m)^2}{2\sigma^2}\right) \quad (1)$$

where H , m , and σ denote the scale, mean, and standard deviation of Gaussian function, respectively. The logarithm of y is calculated as shown in equation (2).

$$\begin{aligned} \log y &= \log H - \frac{1}{2\sigma^2}(x-m)^2 \\ &= -\frac{1}{2\sigma^2}x^2 + \frac{1}{\sigma^2}mx - \frac{m}{2\sigma^2} + \log H \end{aligned} \quad (2)$$

In a variable x sight of view, equation (2) is a second degree polynomial function. In order to estimate the coefficients, we use the least squares approach:

$$E^k = \sum_{i=1}^n \left(\log y_i^k - \left(-\frac{1}{2\sigma^2}(x_i^k)^2 + \frac{1}{\sigma^2}mx_i^k - \frac{m}{2\sigma^2} + \log H \right) \right)^2 \quad (3)$$

where n is number of sample data points, i is the current data point, and k defines the color channel ($k = R, G, B$).

One of the appropriate noise reduction methods for Gaussian distribution is linear smoothing filter such as Gaussian filter. The Gaussian filter for convolution operation is shown as follows:

$$G(x, y) = \frac{1}{2\pi\theta^2} e^{-\frac{x^2+y^2}{2\theta^2}} \quad (4)$$

The SGBNR is applied only if the difference between the center pixel value and its surrounding pixels is less than a defined threshold value. So, the boundary on image such as object edge is efficiently maintained if the appropriate threshold value is selected.

In equation (2), the coefficient σ shows how much dispersion exists from the mean value. Confidence interval means a possible range of same color in a probability sight of view. For a 95 percent confidence interval, four times of standard deviation is selected as a threshold of the SGBNR.

Illumination-Invariant Target Color Detection

The general image acquisition process could be modeled based on Lambertian surface as shown in equation (5) [10,11].

$$\rho_k = B \int E(\lambda) S(\lambda) Q_k(\lambda) d\lambda \quad (5)$$

where ρ_k ($k = R, G, B$) denotes the color values acquired by a camera using the RGB sensors and λ denotes the wavelength, respectively. The spectral sensitivities of the RGB sensors are denoted by $Q_k(\lambda)$ and the spectral power distribution of a light and surface reflectance of an object are denoted by $E(\lambda)$ and $S(\lambda)$, respectively. The B is a constant which is the Lambertian shading term that presents the angle between the surface normal and the illumination direction. Although the EMCCD sensor characteristic is partially bi-modal [12], we suppose that it has uni-modal characteristics in this research.

As we suppose that the delta camera model and Planck's law [10,11], equation (5) can be simply derived as equation (6).

$$\rho_k = B \frac{c_1}{\lambda_k^5} e^{-\frac{c_2}{\lambda_k T}} S(\lambda_k) q_k \quad (6)$$

where B and T denote the scale term and the temperature of a black body, respectively, and c_1 and c_2 are constants defined as $c_1 = 2hc^2$ and $c_2 = hc/k$. Constant c , h and k are denoted as the speed of light (3.0×10^8 (m/s)), the Plank constant (6.626×10^{-34} (Js)) and the Boltzmann constant (1.380×10^{-23} (J/K)), respectively.

In order to reduce the effect of illuminations, RGB values are normalized with the geometric mean ($\sqrt[3]{\rho_R \rho_G \rho_B}$) of the values.

We take the natural logarithm to the normalized values as a preprocessing step to remove an illumination term ' T ', and then we obtain (7).

$$\begin{aligned} \rho'_k &= \ln \left(\frac{\rho_k}{\sqrt[3]{\rho_R \rho_G \rho_B}} \right) \\ &= \ln \left(\frac{\lambda_k^{-5} S(\lambda_k) q_k}{\sqrt[3]{\lambda_R^{-5} S(\lambda_R) q_R \times \lambda_G^{-5} S(\lambda_G) q_G \times \lambda_B^{-5} S(\lambda_B) q_B}} \right) \\ &\quad + \frac{c_2}{T} \left(\frac{(\lambda_R \lambda_G + \lambda_G \lambda_B + \lambda_B \lambda_R)}{3\lambda_R \lambda_G \lambda_B} - \frac{1}{\lambda_k} \right) \end{aligned} \quad (7)$$

Equation (7) can be represented with two vectors as equation (8).

$$\vec{\rho} = \vec{S} + \frac{c_2}{T} \vec{\lambda} \quad (8)$$

To define illumination invariant color space, we remove the c_2/T term. $\vec{\rho}$ is calculated from RGB values of the acquired image. c_2 is a constant, and \vec{S} , $\vec{\lambda}$ and T are unknown variables. To remove the c_2/T term, we apply an inner product with the orthonormal vector of $\vec{\lambda}$, which we denote $\vec{\lambda}^\perp$ ($\vec{\lambda} \cdot \vec{\lambda}^\perp = 0$ and $\|\vec{\lambda}^\perp\| = 1$), to equation (5). Then, we obtain equation (9):

$$\begin{aligned} \vec{\rho} \cdot \vec{\lambda}^\perp &= \left(\vec{S} + \frac{c_2}{T} \vec{\lambda} \right) \cdot \vec{\lambda}^\perp \\ \vec{\rho} \cdot \vec{\lambda}^\perp &= \vec{S} \cdot \vec{\lambda}^\perp \end{aligned} \quad (9)$$

In this case, variance of $\vec{\rho} \cdot \vec{\lambda}$ should be ideally '0', because \vec{S} and $\vec{\lambda}^\perp$ are static for all $\vec{\rho}$ in the training DB. We can estimate $\vec{\lambda}^\perp$ with the training DB, which minimizes variance of $\vec{\rho} \cdot \vec{\lambda}$ by computing equation (10):

$$\arg \min_{\vec{\lambda}^\perp} \left\{ \text{var} \left[\vec{\rho}_i \cdot \vec{\lambda}^\perp \right] \right\} \quad (10)$$

where $\vec{\rho}_i$ denotes the color vector of the i^{th} data in the training DB. Finally, an optimal solution of equation (10) is equation (11).

$$\vec{\lambda}_{opt}^\perp = \left[\frac{1}{\sqrt{1+a^2}} \quad \frac{a}{\sqrt{1+a^2}} \right]^T \quad (11)$$

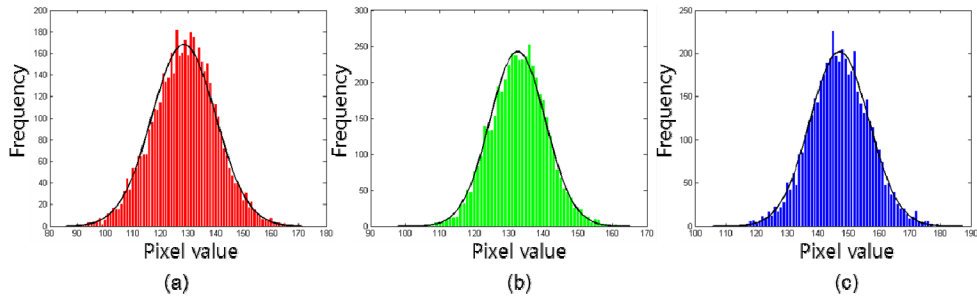


Figure 3. Example of noise modeling (Daylight, 3lx); (a) Red (b) Green and (c) Blue channel

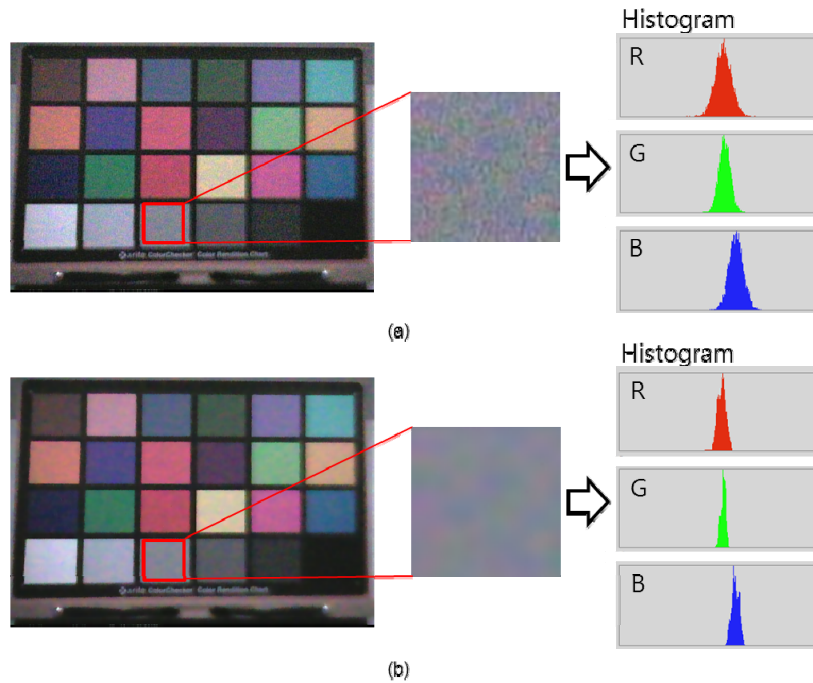


Figure 4. Results of before and after SGBNR; (a) Original image and (b) SGBNR image

Experimental Results

An EMCCD camera (Samsung SHC-750, image size: 704 by 480) and Lens (Samsung MLZ-612AI) are used for the experiment. The color charts employed are GretagMacbeth ColorChecker (24 colors) and GretagMacbeth ColorChecker SG (96 colors) for training and testing, respectively. We obtain the EMCCD images in a lighting booth (X-Rite SpectraLight III) under three kinds of light (Daylight, A, and Horizon) and four low-light-level illuminations (3, 6, 9, and 12 lux).

Table 1 and Fig. 3 show the estimation results of noise analysis. As shown in Fig. 2, noise modeling result (line) fits the patch data (bar) well. Standard deviation (σ) which is shown in Table 1 is used for the threshold of the SGBNR. For example, when the input image is captured in daylight 3 lux conditions, thresholds of each color channel (RGB) for the SGBNR are 46.08, 32.04, and 38.36, respectively. The SGBNR image with those thresholds is shown in Fig. 4. The SGBNR efficiently reduces the EMCCD noise maintaining boundaries.

Table 1. Estimation results of noise analysis (Daylight)

Illumination	Channel	Mean	Standard deviation	H
3 lux	R	128.48	11.52	168.32
	G	132.54	8.01	242.85
	B	147.06	9.59	202.02
6 lux	R	142.04	6.71	290.37
	G	142.99	5.36	360.13
	B	165.04	8.61	230.79
9 lux	R	128.58	5.90	330.49
	G	130.95	4.17	468.14
	B	151.85	6.03	319.09
12 lux	R	138.15	5.26	370.46
	G	140.37	3.99	497.96
	B	159.68	4.57	420.45

Table 2. Estimation results of $\bar{\lambda}_{opt}^\perp$

Colors	Red	Green	Blue	Skin color
$\bar{\lambda}_{opt}^\perp$	$\begin{bmatrix} 0.8007 \\ 0.5991 \end{bmatrix}$	$\begin{bmatrix} 0.7695 \\ 0.6387 \end{bmatrix}$	$\begin{bmatrix} 0.9237 \\ 0.3607 \end{bmatrix}$	$\begin{bmatrix} 0.8934 \\ 0.4493 \end{bmatrix}$

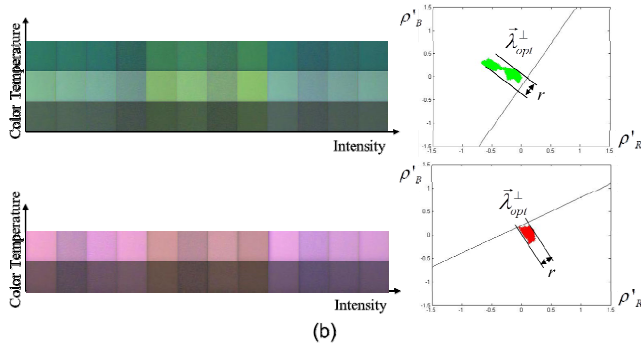
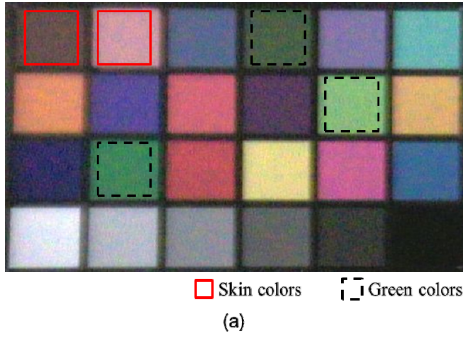


Figure 5. Color patches for training: (a) one of the training images (Daylight, 6 lx) and selected target colors and (b) cropped color patches and their distributions with $\bar{\lambda}_{opt}^\perp$

For the training, we crop the target color patches with 60 by 60 under several illumination conditions as shown in Fig. 5(a). All the options of camera and lens setting are fixed: all functions off, lens f-number 1.4, and no zoom. We obtain $\bar{\lambda}_{opt}^\perp$ vectors from training patches as shown in Table 2 and Fig. 5(b). We select the color detection range (r) by heuristic method (skin: 0.09 ~ 0.32, green: -0.4 ~ -0.02). The color detection range is determined on the vector, $\bar{\lambda}_{opt}^\perp$, and we heuristically selected the range to include the target colors and the origin of the vector depends on the training patch. Representatively green and skin color detection

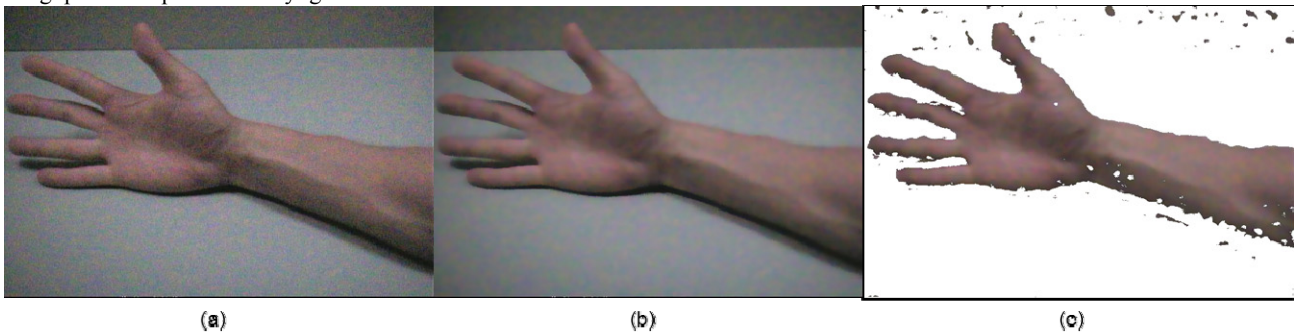


Figure 7. Green and skin color detection results: (a) skin color detection result (A light, 9 lx) and (b) green color detection result (Daylight, 6 lx)

results are shown in Fig. 6. Because skin color is similar with reddish colors, some other colors are detected as a skin color. Fig. 7 shows skin color detection process with intermediate noise reduction result. This image is also captured in the lighting booth (Daylight, 6 lux).

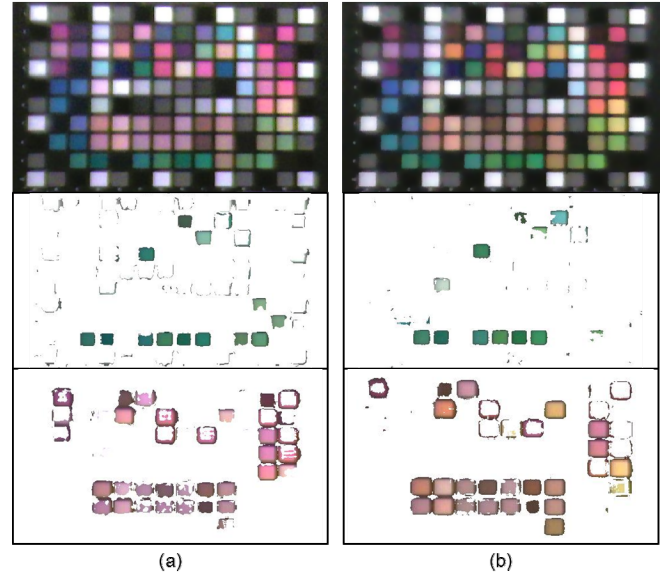


Figure 6. Green and skin color detection results: (a) skin color detection result (A light, 9 lx) and (b) green color detection result (Daylight, 6 lx)

Conclusion

We propose an illumination-invariant target color detection technique with the EMCCD camera for low-light-level conditions. For preprocessing of the EMCCD camera, we reduce the EMCCD noise by using SGBNR method with illumination adaptive threshold. After noise reduction, we experiment target color detection under the several illumination conditions from 3 to 12 (lux) which is similar with dark outdoor situation. Through the experimental results, we show that our target color detection results are robust to low-light-level conditions. This method has a strong advantage of real-time system because the training phase is offline process, and we only use the acquired vector to transform input data into the illumination-invariant color space. It is possible to make an illumination-invariant all day intelligent surveillance system by combining the EMCCD camera with illumination-invariant color space.

References

- [1] P. Jerram, P. Pool, R. Bell, D. Burt, S. Bowring, and S. Spencer, "The LLLCCD: Low Light Imaging without the need for an intensifier," Proc. SPIE, 4306, pg. 178-186, (2001)
- [2] D. J. Denvir and E. Conroy, "Electron Multiplying CCD Technology: The new ICCD," Proc. SPIE, 4796, pg. 167-174, (2003)
- [3] EMCCD technology forum, <http://www.EMCCD.com/>
- [4] P. Jerram, P. Pool, D. Burt, R. Bell, and M. Robbins, "Electron Multiplying CCDs," in SNIC Symposium, pg. 1-5, (2006)
- [5] G. C. Holst and T. S. Lomheim, CMOS/CCD Sensors and Camera Systems, SPIE Press, Bellingham, WA, (2007)
- [6] J. Kriesel and N. Gat, "Performance Tests of True Color Night Vision Cameras," Military Sensing Symposia(MSS) Specialty Group on Passive Sensors, (2006)
- [7] J. Kriesel and N. Gat, "True-color night vision (TCNV) fusion system using a VNIR EMCCD and a LWIR microbolometer camera," Proc. SPIE, 7697, pg. 76970Z 1-8, (2010)
- [8] M. S. Robbins and B. J. Hadwen, "The noise performance of electron multiplying charge-coupled devices," IEEE Trans. on Electron Devices, 50, 5, pg. 1227-1232, (2003)
- [9] GNU Image Manipulation Program, <http://www.gimp.org/>
- [10] U. Yang, B. Kim, K. A. Toh and K. Sohn, "An illumination invariant color space and its application to skin-color detection," Optical Engineering, 49, 10, 107004, (2010)
- [11] G. D. Finlayson, M. S. Drew, and C. Lu, "Intrinsic images by entropy minimization," Lecture Notes in Computer Science: vol. 3023. ECCV 2004: European conference on computer vision, pg. 582-595 (2004)
- [12] M. Kang, U. Yang, and K. Sohn, "Spectral sensitivity estimation for EMCCD camera," IET Electronics Letters, 47, 25, pg. 1369-1370, (2011)

Author Biography

Min-Sung Kang received the B.S. degree from the Department of Electrical and Electronics Engineering in 2006, and currently pursuing his joint M.S./Ph.D. in electronic and electrical engineering from Yonsei University, Korea. His research interests include color image processing, human visual system, and image quality assessment.

Chang-Beom Oh received the B.E. degree in the Department of information and communication engineering from Sejong University, Seoul, Korea in 2011, and currently pursuing his M.S. degree in electronic and electrical engineering from Yonsei University, Seoul, Korea. His research interests include color image processing, and computer vision.

Kwang-Hoon Sohn received the B.E. degree in electronics engineering from Yonsei University, Seoul, Korea in 1983, the MSEE degree in electrical engineering from University of Minnesota, Minneapolis, in 1985, and the Ph.D. degree in electrical and computer engineering from North Carolina State University, Raleigh, in 1992, respectively. Also, he was a Postdoctoral Fellow with the Medical School of Georgetown University, Washington, DC. He is currently a Professor in the School of Electrical and Electronic Engineering, Yonsei University. His research interests include 3-D image processing, computer vision, and image communication.